

Effect of Dissolution of Titanium Ions on Ti Alloys Electrodeposition from EMIC-AlCl₃ Ionic Liquid at Low Temperature



Pravin S. Shinde and Ramana G. Reddy

Abstract In this work, the dissolution of Ti ions from a sacrificial Ti anode during electrolysis on the reduction behavior of Ti–Al alloy electrodeposits from a Lewis acidic eutectic mixture of 1-ethyl-3-methylimidazolium chloride (EMIC) and a 0.667-mol fraction of aluminum chloride (AlCl₃) is investigated. The Ti ions are dissolved in EMIC-AlCl₃ ionic liquid (IL) by potentiostatic and galvanostatic electrolysis using chronoamperometry (CA) and chronopotentiometry (CP) techniques, respectively. At the same time, the electrodeposition of the Ti–Al alloy is accomplished on the copper cathode electrode at 383 K using the Ti anode. The dissolution, concentration, and deposition of Ti species are controlled by varying the electrolysis current, potential, and the electrolysis duration (1–3 h). The electrochemical reduction behavior of Ti and Al ions is studied on all Pt wire electrodes using cyclic voltammetry (CV). SEM studies revealed homogeneous and crystalline Ti–Al electrodeposits for CP-electrolysis. EDS and XRD revealed 16 at %. Ti with a cubic Ti_{0.12}Al_{0.88} phase of Ti–Al alloy obtained from 1 h CP-electrolysis. The Ti content in Ti–Al alloy decreased with an increase in electrolysis time.

Keywords Ti alloy · Electrodeposition · EMIC-AlCl₃ ionic liquid · Electrochemistry · CV · CA · CP

Introduction

Titanium (Ti), because of its highest strength-to-weight ratio, is an essential alloying agent with many metals, including aluminum, molybdenum, and iron. Such alloys find larger applications, including aircraft, spacecraft, and missiles. Because of the excellent corrosion-resistant property, Ti is widely used in medical industries, especially for bone compatibility and surgeries. Ti production by the Kroll process invented in the 1940s has been the known primary method [1]. Despite excellent thermomechanical and corrosion-resistance properties, Ti production is expensive and

P. S. Shinde · R. G. Reddy (✉)

Department of Metallurgical and Materials Engineering, The University of Alabama, Tuscaloosa, AL 35487, USA

e-mail: reddy@eng.ua.edu

difficult to extract and machine [2]. Electrochemical synthesis from low-temperature ionic liquid (IL) electrolytes is one of the fascinating methods of producing Ti metal or its alloys [3]. Unfortunately, the electrochemical mechanism for pure titanium deposition is more complicated than other metals such as aluminum because of its different oxidation states (II, III, and IV). Therefore, it is often electrodeposited in the form of alloys, such as titanium aluminide (Ti-Al). The electrodeposition of Ti and Ti-Al alloys has been performed via an energy-efficient and cost-effective extraction process using the molten chloride salt electrolytes [4–8]. Understanding the electrochemistry of Ti ions in the IL can provide ways to improve the Ti-rich deposition of Ti-Al alloy. The electrochemical studies of TiCl_4 in a strongly Lewis acidic room-temperature molten salt showed that Ti^{4+} is reducible to Ti^{3+} and Ti^{2+} in two steps with one-electron charge transfer each, while Ti^{3+} was deposited at the electrode as a passivating dark thin film layer, mostly as TiCl_3 organic salt [9]. Alternatively, Stafford et al. [10] studied the electrochemistry of titanium using a $2\text{AlCl}_3\text{-NaCl}$ electrolyte in which the oxidation of titanium yielded Ti(II), Ti(III), and Ti(IV) complexes. The divalent species Ti(II) led to electrodeposit Ti-Al alloys, while the trivalent species are sparingly soluble. Despite several attempts to deposit phase-pure Ti, it only resulted in the co-deposition of Al and Ti. Nevertheless, the low-temperature electrochemical synthesis of Ti-Al alloys using IL is not only energy-efficient but also eliminates high-temperature melting and consolidation processes.

The electrodeposition of Ti alloys from chloroaluminate-based alkyl imidazolium chloride IL electrolyte is very challenging because of complex Ti electrochemistry and passivation of electrode surface with the TiCl_3 layer [11–15]. For instance, in an IL of EMIC and AlCl_3 , several anion species such as $[\text{AlCl}_4]^-$, $[\text{Al}_2\text{Cl}_7]^-$, and $[\text{Al}_2\text{Cl}_{10}]^-$ with different concentrations are in equilibrium for a given mole fraction (X_{Al}) of AlCl_3 . The amount of X_{Al} dictates the acidity or basicity of electrolyte and impacts the electrodeposition conditions. At higher AlCl_3 ($X_{\text{Al}} > 0.5$), the electrolyte mainly possesses AlCl_4^- and Al_2Cl_7^- species exhibiting Lewis acidic properties primarily due to coordinately unsaturated Al_2Cl_7^- species [16]. The electrochemical deposition of Al from such chloroaluminate ILs has been reported to be mainly due to contribution from the diffusion of Al_2Cl_7^- species [12, 17, 18]. The electrochemical process of reduction of Al-species in the ILs is relatively well studied. Acidic IL compositions are active for Al plating and stripping at the anode, according to the reversible redox reaction given below [12, 19].



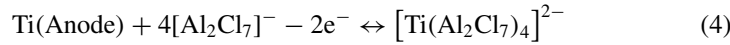
We previously electrodeposited Ti-Al alloys from BMIC- $\text{AlCl}_3\text{-TiCl}_4$ (1:2:0.019 molar ratio) at different applied potentials and temperatures (343–398 K) using Ti foils as cathode and anode, and Ti wire as a reference electrode [20]. The possible reactions are given by Eqs. (2–5).

Cathode reactions:





Anode reactions:



The composition of a solvent-fused salt has a dramatic influence on electrodeposition process of titanium [21–23]. The deposition of pure Ti or its alloy from inorganic and organic melts and ILs is encountered with obstacles of controlling the electrolytes made by dissolving the titanium salts. Addition of salts like TiCl_4 involves its sublimation at elevated temperatures, unwanted disproportionation reaction of titanium ions and formation of passivating TiCl_3 layer resulting into titanium oxide deposition.

To counter most of the mentioned issues, titanium ions can be incorporated into EMIC- AlCl_3 IL by electrochemically controlled dissolution. So far, there are no reports on electrochemical studies on the behavior of dissolution and deposition of Ti species to deposit Ti–Al alloy without the addition of TiCl_4 . In our previous work, the potentiostatic electrodeposition of smooth, compact, and dendrite-free growth of Ti–Al alloy on the copper substrate was demonstrated at -1.3 V versus Ti for 1 h using BMIC- AlCl_3 IL ($X_{\text{Al}} = 0.667$) at low temperature [18]. However, the effect of higher concentrations of Ti species on the Ti–Al deposit compositions was not studied. Furthermore, only the potentiostatic mode was used to dissolve and electrodeposit the Ti–Al alloy.

In this work, it is demonstrated how the dissolution of Ti ions from sacrificial Ti anode during electrolysis and their concentration in the Lewis acidic eutectic ionic liquid mixture of 1-ethyl-3-methylimidazolium chloride and aluminum chloride (EMIC- AlCl_3) affects the electrodeposition behavior of Ti–Al alloy. Then, the electrochemical reduction behavior of Ti and Al ions on Pt wire electrodes is studied using the CV technique by varying the CA and CP-electrolysis durations. The objectives of this research work are to investigate the dissolution and solubility of Ti ions in EMIC- AlCl_3 IL and to determine the underlying reduction mechanism and to characterize surface morphology and composition of the Ti–Al electrodeposits.

Experimental

Preparation of EMIC- AlCl_3 Ionic Liquid

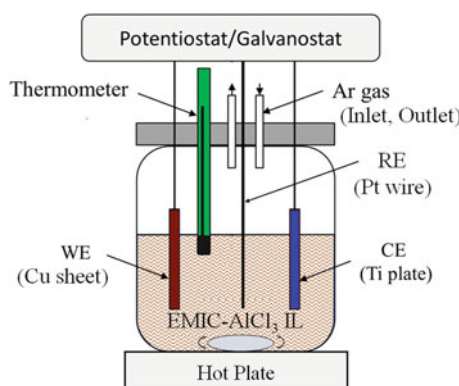
The chemicals such as anhydrous AlCl_3 (95+%, Alfa Aesar) and organic chloride salt 1-ethyl-3-methylimidazolium chloride (EMIC, 95%, Sigma-Aldrich) were

purchased and used without further treatment. The Pt wire (0.5 mm diameter, 99.99%) was obtained from Sigma-Aldrich company. Pure titanium sheet (2 mm thick, 99.99%) was obtained from Alfa Aesar®. The ultrahigh pure (UHP) Argon gas (99.999%) was obtained from Airgas. All chemical reagents were handled in a dry atmosphere. The eutectic mixture of Lewis acidic EMIC-AlCl₃ IL was prepared by mixing a 1:2 molar ratio (AlCl₃ mole fraction, $X_{\text{Al}} = 0.667$) of EMIC and AlCl₃ in a pyrex beaker at room temperature under constant stirring for 30 min until a clear homogeneous solution was obtained. $X_{\text{Al}} = 0.667$ was chosen to maximize the concentration of Al₂Clelectrode as a sacrificial anode – anion species crucial for metal electrodeposition from the EMIC-AlCl₃ IL. The desired amount of clear IL solution is then transferred to the 50 mL electrochemical Pyrex cell placed on a hot plate, and IL was stirred for several minutes using a magnetic stirrer at 60 RPM to achieve a stable temperature of 383 K for further electrochemical studies.

Electrochemical Measurements

All electrochemical measurements were performed from EMIC-AlCl₃ IL at 383 K using cyclic voltammetry (CV), chronoamperometry (CA), and chronopotentiometry (CP) techniques with the help of an EG&G PARC model 273A potentiostat/galvanostat workstation controlled by Power Suite software. The electrochemical cell for the measurements consisted of a 40 mL Pyrex® glass beaker fitted with Teflon/Perspex cover, which has provisions for inserting the electrodes, thermometer, and inert gas inlet/outlets, as shown schematically in Fig. 1. A conventional three-electrode cell (Fig. 1) was used for these measurements. The Ti ions are hard to dissolve in EMIC-AlCl₃ ionic liquid even after putting a Ti slab in it at 383 K. Therefore, the electrolysis approach was chosen to dissolve Ti ions from the metallic Ti counter electrode as a sacrificial anode electrode and incorporate in the EMIC-AlCl₃ IL. The dissolution of Ti ions to deposit Ti-Al alloy was performed by potentiostatic

Fig. 1 Schematic of the experimental setup for CA- and CP-electrolysis from EMIC-AlCl₃ IL. (Color figure online)



(constant potential) and galvanostatic (constant current) electrolysis for different durations (1, 2, and 3 h) using CA and CP techniques, respectively. For electrolysis, copper sheet ($2 \times 2 \times \sim 0.25$ cm, 99%, Sigma-Aldrich) served as working electrode (WE), Ti plate ($2 \times 2 \times \sim 2$ cm, 99.99%, Sigma-Aldrich) served as the counter electrode (CE), and Pt wire (0.05 cm diameter, >99.99%, Alfa Aesar) as a quasi-reference electrode (q-RE). The CV measurements were performed before and after CA-electrolysis, and after CP-electrolysis using all Pt electrodes as WE, CE, and q-RE. The working distance between WE and CE was 2 cm. The temperature was controlled by a hot plate and was precisely monitored by the inserted thermometer. The Ar gas flow was continuously maintained through the alumina tube during the experiment.

Before electrochemical measurements, all the electrodes were polished with 800-grit SiC abrasive paper, rinsed thoroughly with deionized water, cleaned in an ultrasonic bath for 5 min, and dried by air to remove any residual impurities. The height of the electrodes immersed in the IL was measured after each experiment. Ti-Al alloy was deposited on copper plate by CA-electrolysis from EMIC-AlCl₃ ($X_{\text{Al}} = 0.667$) IL electrolyte at 383 K at a fixed applied potential of -1.5 V versus Pt and by CP-electrolysis at 10 mA cm^{-2} for 1, 2, and 3 h durations. The electrodeposited Ti-Al alloy electrodes were characterized using structural, morphological, and compositional techniques such as scanning electron microscopy (SEM) on Thermo Scientific™ Apreo scanning electron microscope equipped with energy dispersive spectroscopy (EDS), and X-ray diffraction (XRD) on a Bruker D8 Discover X-ray diffractometer with GADDS by employing monochromatic Co K α radiation.

Results and Discussion

Cyclic Voltammetry of Ti-Free EMIC-AlCl₃ IL

The cyclic voltammetry is used to study the electron transfer process for Al deposition from freshly prepared EMIC-AlCl₃ IL at different scan rates before potentiostatic CA-electrolysis to dissolve Ti ions. A standard three-electrode configuration cell with three Pt wires was used as working, counter, and quasi-reference electrodes.

Figure 2a shows a typical CV recorded from EMIC-AlCl₃ IL ($X_{\text{Al}} = 0.667$) on a polished Pt wire electrode at 383 K. The potential is swept at 300 mV s^{-1} from open-circuit potential (OCP) to -2.0 V versus Pt, where Al (III)-complex [Al₂Cl₇]⁻ ions are reduced to Al (0) and then reversed back to OCP. The electrodeposition (reduction) of Al commences at -1.34 V versus Pt and reaches the maximum current at -1.75 V. After this peak potential, the current decreases until the reversal of potential, indicating the drop in the concentration of electroactive Al₂Cl₇⁻ species near the electrode. During the anodic potential sweep, the occurrence of a broad stripping peak at -0.64 V corresponds to the oxidation of the Al (0) electrodeposited during the cathodic sweep. Additionally, the CV shows the distinct redox peaks in

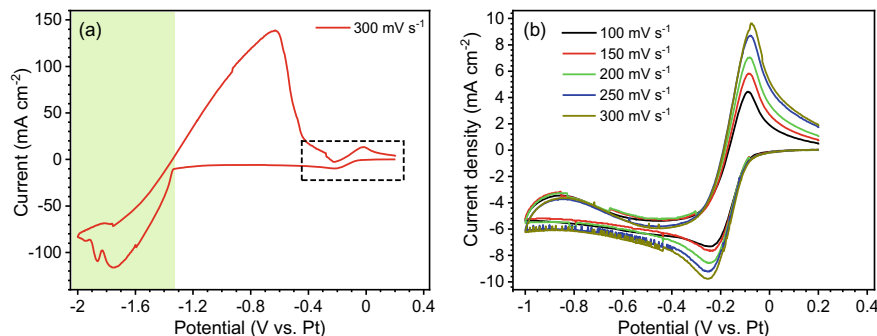


Fig. 2 **a** A typical CV recorded on polished Pt wire from EMIC-AlCl₃ IL at the scan rate of 300 mV s⁻¹ at 383 K showing cathodic deposition of Al and its subsequent anodic stripping during the reverse direction. **b** CV curves recorded in the potential range from OCP to -1 V versus Pt at different scan rates (100–300 mV s⁻¹), indicating UPD deposition and stripping of Al. (Color figure online)

the potential range from 0 to -0.8 V. It is reported that Ti can be reduced (from Ti⁴⁺ to Ti²⁺) from Ti-containing chloroaluminate ionic liquid in the potential from 0 to -1.0 V versus Pt [24]. Hence, the CV curves were recorded from EMIC-AlCl₃ IL with and without Ti ions dissolved electrochemically by CA and CP modes at different hours. Figure 2b shows the CV curves recorded from Ti-free EMIC-AlCl₃ IL at different scan rates (100–300 mV s⁻¹) at 383 K. Please note that these CVs were recorded before recording the extended CV shown in Fig. 1a. The potential is varied from open-circuit potential to -1.0 V versus Pt. The CVs show a cathodic peak at -0.25 V versus Pt, which can be ascribed to the underpotential deposition (UPD) of aluminum, and its corresponding counterpart anodic peak on the reverse scan at -0.08 V versus Pt is attributed to stripping of UPD Al. Similar UPD behavior is observed by several researchers [25–27]; however, the mechanism of UPD is still unclear. It is reported that UPD is responsible for nanocrystalline growth of Al, while the broader redox peaks followed by UPD are responsible for microcrystalline or bulk growth of Al in the electrodeposit [26].

Electrochemical Dissolution of Ti Ions by CA-Electrolysis

After recording CVs from EMIC-AlCl₃ IL, the Ti ions were incorporated into it employing electrolysis using a pure Ti plate as anode and Cu sheet as a cathode. The two methods of electrolysis, potentiostatic chronoamperometry (CA) and galvanostatic chronopotentiometry (CP), were employed at different durations. The cathode and anode electrodes were weighed before and after each electrolysis to account for the amount of Ti ions stripped from the Ti anode and the amount of Ti-Al material deposited onto the Cu cathode electrode.

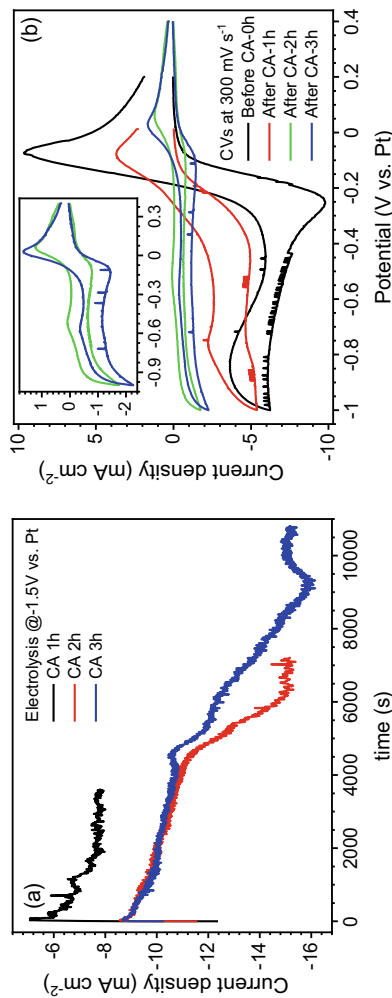


Fig. 3 **a** CA-electrolysis curves for 1, 2, and 3 h durations on Cu cathode at -1.5 V versus Pt. **b** Overlay of representative CVs recorded before and after CA-electrolysis for different durations at 300 mV s^{-1} at 383 K. The inset shows the magnified view of CV curves recorded for 2 and 3 h CA-electrolysis time. (Color figure online)

Table 1 Weight gain and loss of Cu cathode and Ti anode electrodes during CA and CP-electrolysis at different times

| Electrolysis mode | Duration (h) | Weight gain of Cu cathode due to Ti-Al deposition (Wt.%) | Weight loss of Ti anode due to the stripping of Ti ions (Wt.%) |
|-------------------|--------------|--|--|
| CA | 1 | 0.25 | 0.57 |
| CA | 2 | 2.34 | 2.05 |
| CA | 3 | 3.05 | 3.40 |
| CP | 1 | 0.89 | 0.78 |
| CP | 2 | 2.85 | 1.82 |
| CP | 3 | 2.97 | 2.90 |

Figure 3a shows CA-electrolysis curves for 1, 2, and 3 h durations carried out independently with identical experimental conditions. The current density increases over time. The current density rises sharply after about 75 min as seen for 2 and 3 h CA-electrolysis. Electrolyte temperature plays role in shifting the deposition potential to less negative values. Rise in temperature of the EMIC-AlCl₃ IL causes increase in mobility of the electroactive [Al₂Cl₇]⁻ and Ti[(Al₂Cl₇)₄]²⁻ species toward the Cu cathode electrode surface leading to an increase of the reaction rate. The reason for temperature rise due to exothermic electrochemical reactions during higher electrolysis durations needs to be investigated. In general, the conductivity and viscosity of ionic liquids are strongly dependent on temperature [28]. The weight loss and gain percentages of Ti anode and Cu cathode with varying CA-electrolysis time are shown in Table 1. The wt. % of Cu cathode increases with electrolysis time, due to the Ti-Al deposition. At the same time, the Ti ions released by Ti anode in EMIC-AlCl₃ IL increases with time as indicated by wt. % loss of Ti anode.

Figure 3b shows the representative CVs recorded in separate experiments before and after CA-electrolysis for different durations at 300 mV s⁻¹ at 383 K. Before CA-electrolysis, the typical UPD redox peaks are seen. However, with the increasing duration of CA-electrolysis, the current density of UPD peaks decreases. Moreover, new redox peaks emerge in the potential range from -0.9 to -0.7 V versus Pt, which corresponds to the deposition of Ti species (reduction of Ti₄₊ to Ti₂₊). The current density for Ti peaks (along with UPD Al) decreases with CA-electrolysis time despite the continuous release of Ti ions in IL, suggesting a saturation limit to form the Ti complex with [Al₂Cl₇]⁻ ions. As a result, despite the higher concentration of Ti ions released in IL by Ti anode, significantly less Ti[(Al₂Cl₇)₄]²⁻ ions are available for co-electrodeposition of Ti along with Al. The primary electrodeposition process proceeds at more negative potentials to deposit microcrystalline or bulk Al (around -1.5 V vs. Pt).

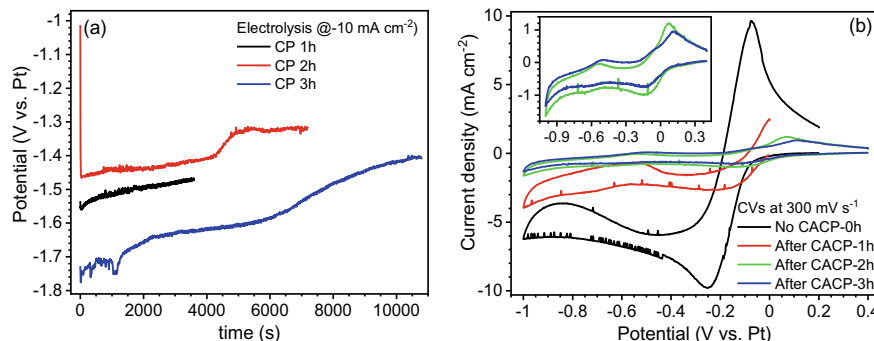


Fig. 4 **a** CP-electrolysis curves for 1, 2, and 3 h durations on Cu cathode at a constant current density. **b** Overlay of representative CVs recorded before and after CA-electrolysis for different durations at 300 mV s^{-1} at 383 K. The inset shows the magnified view of CV curves recorded for 2 and 3 h CP-electrolysis time. (Color figure online)

Electrochemical Dissolution of Ti Ions by CP-Electrolysis

After recording CA-electrolysis, the CP electrolysis was performed from Ti-enriched EMIC- AlCl_3 IL using a fresh Ti plate as anode and Cu sheet as a cathode.

Figure 4a shows the CP-electrolysis curves for 1, 2, and 3 h durations carried out independently with identical experimental conditions. The potential fluctuates initially in the range of -1.45 and -1.75 V versus Pt and decreases over time as the more TiA-I gets deposited on the Cu cathode. Figure 4b shows the representative CVs recorded in separate experiments before and after CA and CP-electrolysis for different durations at 300 mV s^{-1} at 383 K. Similar to CA-electrolysis, the current density of UPD Al and Ti decreases with the increasing duration of CP-electrolysis. However, the Ti redox peaks are more evident in the potential range from -0.9 to -0.7 V versus Pt (see inset of Fig. 4b). Again, a drop in current density could be due to the availability of limited concentration of $\text{Ti}[(\text{Al}_2\text{Cl}_7)_4]^{2-}$ ions, and CP electrolysis is driven mainly by Al deposition at higher electrolysis time.

Morphological and Compositional Analysis by SEM-EDS

SEM and EDS analyses were performed to examine the morphology and chemical composition of the electrodeposits. Figure 5abc shows SEM images of Ti-Al electrodeposits obtained from CA-electrolysis. For 1 h, the Ti-Al electrodeposit shows uniform coverage of large grains with several cracks. With increasing time, the crack disappears, forming a continuous layer. Homogeneous and smooth deposits are seen for 3 h. The morphology of Ti-Al deposits obtained by CP-electrolysis is compact and crystalline (Fig. 5def). Ti-Al deposit from 3 h CP-electrolysis reveals 2–3 μm size

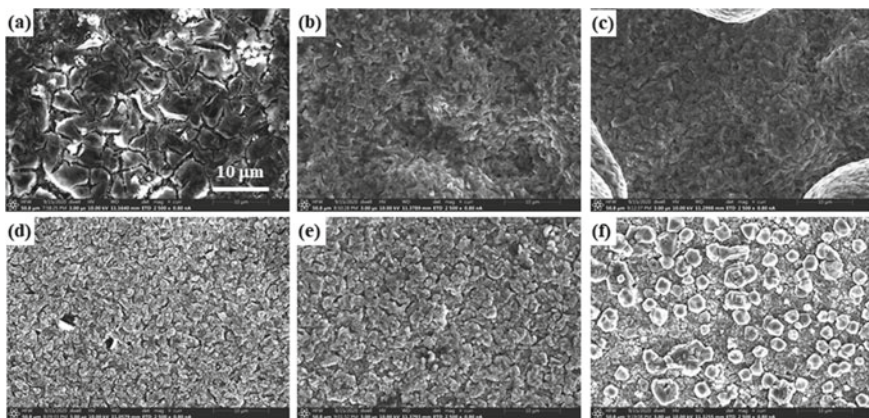


Fig. 5 Surface morphologies of Ti-Al alloys on Cu substrate by potentiostatic electrodeposition for **a** 1 h, **b** 2 h, and **c** 3 h, and galvanostatic electrodeposition for **d** 1 h, **e** 2 h, and **f** 3 h. Magnification: 2500X

grains crystallized on top of the continuous Ti-Al layer. Such crystallization could be due to a rise in temperature of the EMIC-AlCl₃ IL due to exothermic reaction.

Figure 6 shows the EDS spectra obtained from a selected area (2500X) of Ti-Al electrodeposits obtained from CA- and CP-electrolysis for different durations. As

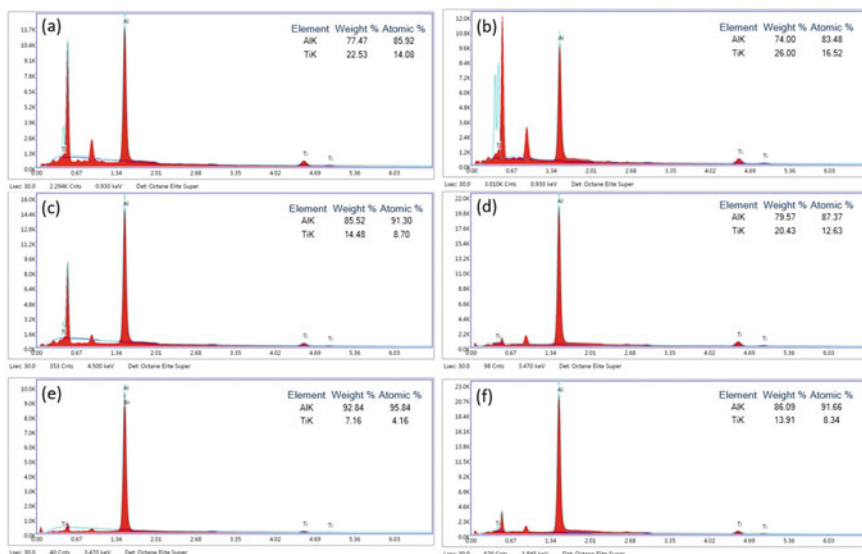


Fig. 6 EDS analysis on a selected area (2500X magnification) of Ti-Al electrodeposits obtained from CA-electrolysis for **a** 1 h, **c** 2 h, and **e** 3 h and from CP-electrolysis for **b** 1 h, **d** 2 h, and **f** 3 h. The inset shows the percentage composition of Ti and Al elements. (Color figure online)

seen from Fig. 6ace, the chemical compositions of Ti and Al in Ti–Al electrodeposit from 1 h CA-electrolysis are 14 at.% and 86 at.%, respectively. The atomic percentage of Ti goes on decreasing with increasing CA-electrolysis time. Ti–Al electrodeposits obtained by CP-electrolysis show relatively higher concentrations of Ti (16.5 at.%), understandably due to the higher concentration of Ti ions dissolved in EMIC- AlCl_3 . However, Ti concentration goes on decreasing with increasing CP-electrolysis time. The decrease in Ti concentration in the EDS spectrum at higher CA- and CP-electrolysis time agrees with the drop in the current density for UPD Al and Ti peaks, as discussed earlier in the CV section.

Structural Analysis by XRD

The Ti–Al electrodeposits were further characterized using XRD. Figure 7 shows the normalized XRD patterns of Ti–Al electrodeposits obtained on Cu substrate from CA-electrolysis (CA1, CA2, and CA3) and CP-electrolysis (CP1, CP2, and CP3). XRD of all the electrodeposits shows five distinct crystallographic peaks of Ti–Al identified according to PDF4+ card (ICDD#04-016-6423), while the rest of the peaks are due to copper substrate. The five crystallographic planes (111), (200), (220), (311), and (222) belongs to the cubic $\text{Ti}_{0.12}\text{Al}_{0.88}$ phase (space group: Fm-3 m (225)) of Ti–Al alloy. No other peaks of metallic elements are detected. The atomic percentage composition observed from XRD agrees with the EDS studies. The intensity of (220) and (311) planes increases with increasing electrolysis time for CA as well as CP-electrolysis. The Ti–Al (CP3 sample) electrodeposit obtained

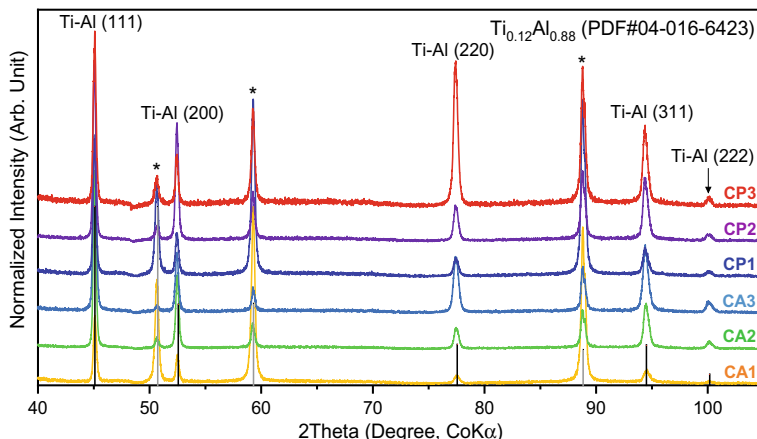


Fig. 7 XRD patterns of Ti–Al electrodeposits obtained from EMIC- AlCl_3 on the copper substrate by CA-electrolysis (1–3 h) and CP-electrolysis (1–3 h). The vertical lines represent the lines from standard diffraction patterns of Ti–Al alloy ($\text{Ti}_{0.12}\text{Al}_{0.88}$) and Cu(*). (Color figure online)

from CP-electrolysis for 3 h shows the highest crystallinity and agrees with the morphological SEM study.

Thus, through this work, we demonstrated that it is feasible to synthesize Ti–Al alloy by dissolving Ti ions in the ionic liquid from Ti anode during electrolysis. It is crucial to investigate the solubility limitations in the reduction of Ti complex ions at higher electrolysis duration. More work is needed to understand the Ti electrochemistry and the disproportionate behavior of Ti ions. Future work is to improve the Ti content in Ti–Al alloy by tailoring the CA and CP-electrolysis parameters.

Conclusions

The dissolution of Ti ions from Ti anode in EMIC-AlCl₃ (with a 0.667-mol fraction of AlCl₃) ionic liquid at 383 K is investigated. The simultaneous dissolution of Ti ions and electrodeposition of Ti–Al alloy on the copper cathode is accomplished by controlled electrolysis using chronoamperometry and chronopotentiometry techniques at different durations. The electrochemical reduction behavior of Ti and Al ions is studied on all Pt wire electrodes using cyclic voltammetry. The reduction of Ti ions commences along with the underpotential deposition of Al. The Ti content in Ti–Al alloy goes on decreasing with higher electrolysis time using CA and CP methods. This indicates that the reduction current of Ti ions is limited by the formation of Ti complex with [Al₂Cl₇][−] anions present in the EMIC-AlCl₃ ionic liquid. The Ti–Al electrodeposits obtained from CP-electrolysis are homogeneous and crystalline. One-hour CP-electrolysis yields a Ti–Al alloy with 16 at.% Ti with a cubic Ti_{0.12}Al_{0.88} phase.

Acknowledgements The authors acknowledge the financial support from the National Science Foundation (NSF) award number 1762522 and ACIPCO for this research project. The authors also thank the Department of Metallurgical and Materials Engineering, The University of Alabama, for providing the experimental and analytical facilities.

References

1. Kroll W (1940) The production of ductile titanium. *Trans Electrochem Soc* 78:35
2. Crowley G (2003) How to extract low-cost titanium. *Adv Mater Processes* 161:25–27
3. Zhang M, Kamavaram V, Reddy RG (2006) Ionic liquid metallurgy: novel electrolytes for metals extraction and refining technology. *Mining Metall Explor* 23:177–186
4. Fung KW, Mamantov G (1972) Electrochemistry of titanium (II) in AlCl₃-NaCl melts. *J Electroanal Chem* 35:27–34
5. Girginov A, Tsvetkov TZ, Bojinov M (1995) Electrodeposition of refractory-metals (Ti, Zr, Nb, Ta) from molten-salt electrolytes. *J Appl Electrochem* 25:993–1003
6. Rolland W, Sterten A, Thonstad J (1987) Electrodeposition of titanium from chloride melts. *Proc Electrochem Soc* 7:775–785

7. Head RB (1961) Electrolytic production of sintered titanium from titanium tetrachloride at a contact cathode. *J Electrochem Soc* 108:806–809
8. Stafford GR (1994) The electrodeposition of Al_3Ti from chloroaluminate electrolytes. *J Electrochem Soc* 141:945–953
9. Carlin RT, Osteryoung RA, Wilkes JS, Rovang J (1990) Studies of titanium (IV) chloride in a strongly Lewis acidic molten-salt-electrochemistry and titanium NMR and electronic spectroscopy. *Inorg Chem* 29:3003–3009
10. Stafford GR, Moffat TP (1995) Electrochemistry of titanium in molten $2AlCl_3-NaCl$. *J Electrochem Soc* 142:3288–3296
11. Koronaios P, King D, Osteryoung RA (1998) Acidity of neutral buffered 1-Ethyl-3-methylimidazolium chloride- $AlCl_3$ ambient-temperature molten salts. *Inorg Chem* 37:2028–2032
12. Jiang T, ChollierBrym MJ, Dubé G, Lasia A, Brisard GM (2006) Electrodeposition of aluminium from ionic liquids: part I—Electrodeposition and surface morphology of aluminium from aluminium chloride ($AlCl_3$)-1-ethyl-3-methylimidazolium chloride ([EMIm]Cl) ionic liquids. *Surf Coat Technol* 201:1–9
13. Kamavaram V, Mantha D, Reddy RG (2005) Recycling of aluminum metal matrix composite using ionic liquids: effect of process variables on current efficiency and deposit characteristics. *Electrochim Acta* 50:3286–3295
14. Liao Q, Pitner WR, Stewart G, Hussey CL, Stafford GR (1997) Electrodeposition of aluminum from the aluminium chloride-1-methyl-3-ethylimidazolium chloride room temperature molten salt + benzene. *J Electrochem Soc* 144:936–943
15. Zhao Y, VanderNoot T (1997) Electrodeposition of aluminium from room temperature $AlCl_3$ -TMPAC molten salts. *Electrochim Acta* 42:1639–1643
16. Karpinski ZJ, Osteryoung RA (1984) Determination of equilibrium-constants for the tetra-chloroaluminate ion dissociation in ambient-temperature ionic liquids. *Inorg Chem* 23:1491–1494
17. Pradhan D, Reddy RG (2014) Mechanistic study of Al electrodeposition from EMIC- $AlCl_3$ and BMIC- $AlCl_3$ electrolytes at low temperature. *Mater Chem Phys* 143:564–569
18. Tang J, Azumi K (2011) Optimization of pulsed electrodeposition of aluminum from $AlCl_3$ -1-ethyl-3-methylimidazolium chloride ionic liquid. *Electrochim Acta* 56:1130–1137
19. Wilkes JS, Levisky JA, Wilson RA, Hussey CL (1982) Dialkylimidazolium chloroaluminate melts—a new class of room-temperature ionic liquids for electrochemistry, spectroscopy, and synthesis. *Inorg Chem* 21:1263–1264
20. Pradhan D, Reddy RG (2009) Electrochemical production of Ti-Al alloys using $TiCl_4$ - $AlCl_3$ -1-Butyl-3-Methyl imidazolium chloride (BmimCl) electrolytes. *Electrochim Acta* 54:1874–1880
21. Song J, Wang Q, Wu J, Jiao S, Zhu H (2016) The influence of fluoride ions on the equilibrium between titanium ions and titanium metal in fused alkali chloride melts. *Faraday Discuss* 190:421–432
22. Song J, Xiao J, Zhu H (2017) Electrochemical behavior of titanium ions in various molten alkali chlorides. *J Electrochem Soc* 164:E321
23. Song Y, Jiao S, Hu L, Guo Z (2016) The cathodic behavior of Ti (III) Ion in a $NaCl$ - $2CsCl$ Melt. *Mettall Mater Trans B* 47:804–810
24. Endres F, Zein El Abedin S, Saad AY, Moustafa EM, Borissenko N, Price WE, et al. (2008) On the electrodeposition of titanium in ionic liquids. *PhysChemChemPhys* 10:2189–2199
25. Bakkar A, Neubert V (2015) A new method for practical electrodeposition of aluminium from ionic liquids. *Electrochim Commun* 51:113–116
26. Zein El Abedin S, Giridhar P, Schwab P, Endres F (2010) Electrodeposition of nanocrystalline aluminium from a chloroaluminate ionic liquid. *Electrochim Commun* 12:1084–1086
27. Böttcher R, Valitova A, Ispas A, Bund A (2019) Electrodeposition of aluminium from ionic liquids on high strength steel. *Trans IMF* 97:82–88
28. Okoturo OO, VanderNoot TJ (2004) Temperature dependence of viscosity for room temperature ionic liquids. *J Electroanal Chem* 568:167–181